SCIENTIFIC REPORTS

OPEN

MHD flow of Maxwell fluid with nanomaterials due to an exponentially stretching surface

Umer Farooq[1,2], Dianchen Lu[1], Shahzad Munir[2], Muhammad Ramzan[3,4], Muhammad Suleman[1,2] & Shahid Hussain[5]

In many industrial products stretching surfaces and magnetohydrodynamics are being used. The purpose of this article is to analyze magnetohydrodynamics (MHD) non-Newtonian Maxwell fluid with nanomaterials in a surface which is stretching exponentially. Thermophoretic and Brownian motion effects are incorporated using Buongiorno model. The given partial differential system is converted into nonlinear ordinary differential system by employing adequate self-similarity transformations. Locally series solutions are computed using BVPh 2.0 for wide range of governing parameters. It is observed that the flow is expedite for higher Deborah and Hartman numbers. The impact of thermophoresis parameter on the temperature profile is minimal. Mathematically, this study describes the reliability of BVPh 2.0 and physically we may conclude the study of stretching surfaces for non-Newtonian Maxwell fluid in the presence of nanoparticles can be used to obtain desired qualities.

Heat transfer and magnetohydrodynamics in the boundary layer flows are important research topics due to their usage in industry and metallurgy. Several procedures such as chilling of filaments or continuous strips by taking them out from stagnant fluid involve stretching of these strips. The refrigeration of temperature reduction finally defines the quality of the end product. Further such flows are important in view of engineering applications related to geothermal energy extractions, crystal growing, power plants, plasma studies, paper production and MHD generators. Sakiadis[1–3] presented pioneering research on flow induced by stretching surface. Afterwards, the problems for linear and nonlinear stretching surfaces have been investigated extensively (see for instance)[4–6]. Pioneer research on the flow due to an exponentially stretching surface was done by Magyari and Keller[7]. Sajid and Hayat[8] discussed the importance of thermal radiation. Sahoo and Poncet[9] studied partial slip effect for the third grade fluid flow. Mukhopadhyay investigated porous medium and thermally stratified medium in an exponentially stretching surface[10,11]. Rahman et al.[12] addressed such flow considering second order slip by utilizing Buongiorno's model. Hayat et al.[13] developed analysis for Oldroyd-B fluid. Patil et al.[14] obtained non-similar solutions for such flows for stretching surface considering mixed convection, double diffusion and viscous dissipation effects. Few other studies with reference to the flow and heat transfer characteristics of viscous and non-viscous fluids over surfaces which are stretching exponentially can be found through the refs therein[15–23].

The studies related to non-Newtonian fluids have generated considerable interest in recent times. This is as a result of their numerous utilizations in industrial products. In general, such fluids cannot be explained by one constitutive equation. Hence, different constitutive equations are proposed in view of the diversity of such fluids. Fluids of non-Newtonian types are mainly distributed among integral, rate and differential types. Maxwell fluid falls under rate type non-viscous fluids category. This class illustrates the relaxation time effects. In past, Fetecau[24] obtained exact solution for Maxwell fluid flow. Wang and Hayat[25] studied Maxwell fluid flow in porous medium. Fetecau et al.[26] investigated fraction Maxwell fluid for unsteady flow. Hayat et al.[27] studied two-dimensional MHD Maxwell fluid. Heyhat and Khabzi[28] investigated MHD upper-convected Maxwell (UCM) fluid flow above a flat rigid region. Hayat and Qasim[29] obtained series solutions for two-dimensional MHD flow with thermophoresis

[1]Department of Mathematics, Faculty of Science, Jiangsu University, 212013, Zhenjiang, China. [2]Department of Mathematics, COMSATS University Islamabad, Park road, Tarlai Kalan, 44000, Islamabad, Pakistan. [3]Department of Mechanical Engineering, Sejong University, Seoul, 143-747, Korea. [4]Department of Computer Science, Bahria University, Islamabad Campus, Islamabad, 44000, Pakistan. [5]School of Materials Science and Engineering, Jiangsu University, Zhenjiang, 212013, China. Shahzad Munir, Muhammad Ramzan, Muhammad Suleman and Shahid Hussain contributed equally. Correspondence and requests for materials should be addressed to U.F. (email: umer_farooq@comsats.edu.pk) or D.L. (email: dclu@ujs.edu.cn)
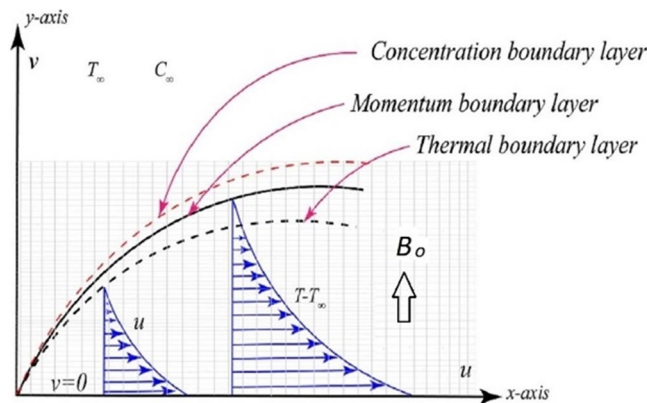
Figure 1. Physical Configuration.

and Joule heating. Jamil and Fetecau[30] considered Maxwell fluid for Helical flows between coaxial cylinders. Zheng et al.[31] constructed closed form solutions for generalized Maxwell fluid in a rotating flow. Wang and Tan[32] presented stability analysis for Maxwell fluid subject to double-diffusive convection, porous medium and soret effects. Motsa et al.[33] examined UCM flow in a porous structure. Mukhopadhyay et al.[34] elaborated thermally radiative Maxwell fluid flow over a continuously permeable expanding surface. Ramesh et al.[35] numerically investigated Maxwell fluid with nanomaterials for MHD flow in a Riga plate. Ijaz et al.[36] explored the behavior of Maxwell nanofluid flow for the motile gyrotactic microorganism in magnetic field. UCM fluid model for non-Fourier heat flux is investigated by Ijaz et al.[37].

Nanofluids consists of ordinary liquids and nanoparticles. Nanofluids are quite useful to improve the performance of ordinary liquids. Nanofluids are developed by inserting fibers and nanometer size particles to original fluids. Nanofluids are especially significant in hybrid powered engines, pharmaceutical processes, fuel cells, microelectronics. The nanoparticles basically connect atomic structures with bulk materials. Commonly used ordinary liquids include toluene, oil, water, engine oil and ethylene glycol mixtures. The metal particles include aluminum, titanium, gold, iron or copper. The nanofluids commonly contains up to 5% fraction volume of nanoparticles to obtain significant improvement in heat transfer. Further, the magnetic nanofluids have great interest in optical switches, biomedicine, cancer therapy, cell separation, optical gratings and magnetic resonance imaging. An extensive review on nanofluids includes the attempts of[38,39]. One can also mention the previous recent studies[40–45] regarding the improvement of thermal conductivity in the nanofluids.

In view of aforementioned discussion, the MHD flow of non-viscous Maxwell fluid with nanomaterials in an exponentially stretching surface is addressed. The BVPh 2.0 which is developed on the basis of optimal homotopy analysis method (OHAM) is employed to solve nonlinear differential system[46–50]. The convergence of the present results is discussed by the so-called average squared residual errors. Velocity, temperature, concentration, the local Sherwood and the local Nusselt number are also examined through graphs.

Problem Formulation

Figure 1 describes the MHD laminar, incompressible flow, thermal and concentration boundary layers in a surface which is stretching exponentially with velocity U_w and given concentration C_w and temperature T_w is described using boundary layer theory as follows:

$$\frac{\partial u}{\partial x} + \frac{\partial v}{\partial y} = 0, \tag{1}$$

$$u\frac{\partial u}{\partial x} + v\frac{\partial u}{\partial y} = \nu\frac{\partial^2 u}{\partial x^2} - \lambda\left[u^2\frac{\partial^2 u}{\partial x^2} + 2uv\frac{\partial^2 u}{\partial x\partial y} + v^2\frac{\partial^2 u}{\partial y^2}\right] - \frac{\sigma B_o^2}{\rho_f}\left(\lambda v\frac{\partial u}{\partial y} + u\right), \tag{2}$$

$$u\frac{\partial T}{\partial x} + v\frac{\partial T}{\partial y} = \alpha\frac{\partial^2 T}{\partial y^2} + \tau\left\{\frac{D_T}{T_\infty}\left(\frac{\partial T}{\partial y}\right)^2 + D_B\left(\frac{\partial C}{\partial y}\frac{\partial T}{\partial y}\right)\right\}, \tag{3}$$

$$u\frac{\partial C}{\partial x} + v\frac{\partial C}{\partial y} = D_B\left(\frac{\partial^2 C}{\partial y^2}\right) + \frac{D_T}{T_\infty}\left(\frac{\partial^2 T}{\partial y^2}\right). \tag{4}$$

where, u is the x component and v is the y component of the Maxwell fluid velocity. Also g, D_T, C, T_∞, λ, ν, ρ_f, C_∞, T, σ, D_B and α represents gravitational acceleration, thermophoretic diffusion coefficient, nanoparticle volume fraction, free stream temperature, relaxation time, the ratio between nanoparticle and original fluids

heat capacities, kinematic viscosity, fluid density, free stream concentration, temperature, electrical conductivity, Brownian diffusion coefficient and thermal diffusivity, respectively. The subjected boundary conditions (BCs) are given by,

$$U_w(x) = u = U_0 exp\left(\frac{x}{l}\right), \quad T_w = T = T_\infty + T_0 exp\left(\frac{x}{2l}\right), \quad v = 0, \tag{5}$$

$$C_w = C = C_\infty + C_0\, exp\left(\frac{x}{2l}\right) \text{ at } y = 0, \tag{6}$$

$$u \to 0, \quad C \to C_\infty, \quad T \to T_\infty, \quad v \to 0 \quad \text{as} \quad y \to \infty. \tag{7}$$

The adequate transformations for the considered problem are taken as follows:

$$\eta = \sqrt{\frac{U_0}{2\nu l}}\, exp\left(\frac{x}{2l}\right)y, \quad \psi = \sqrt{2l\nu U_0}\, f(\eta)exp\left(\frac{x}{2l}\right), \quad uU_0 exp\left(\frac{x}{l}\right)f'(\eta),$$

$$v = \sqrt{\frac{U_0\nu}{2l}}\, exp\left(\frac{x}{2l}\right)[\eta f'(\eta) + f(\eta)], \quad \theta(\eta) = \frac{T - T_\infty}{T_0\, exp\left(\frac{x}{2l}\right)}, \quad \phi(\eta) = \frac{C - C_\infty}{C_0\, exp\left(\frac{x}{2l}\right)}. \tag{8}$$

Substitution of (8) into (2)–(4) yields

$$f''' - 2f'^2 - 2M^2 f' + \beta\left(3ff'f'' + \frac{\eta}{2}(f')^2 f'' - 2(f')^3 - \frac{1}{2}f^2 f'''\right)$$
$$+ M^2\beta(\eta f'f'' + ff'') + ff'' = 0, \tag{9}$$

$$\theta'' + Pr(f\theta' + N_t\theta'^2 - f'\theta + N_b\theta'\phi') = 0, \tag{10}$$

$$\phi'' + \frac{N_t}{N_b}\theta'' - PrLe(f'\phi - f\phi') = 0, \tag{11}$$

in which the incompressibility condition (1) is satisfied identically and the parameters Le, M, N_b, β, Pr, N_t are the Lewis number, Hartman number, the Brownian motion parameter, Deborah number, Prandtl number and the thermophoresis parameter, respectively. The definitions of these numbers are,

$$M^2 = \frac{\rho B_0^2 l}{\rho U_w}, \ \ \beta = \frac{\lambda U_w}{l}, \ \ N_t = \frac{\tau D_T T_0 exp(x/2l)}{\nu T_\infty}, \ \ Le = \frac{\alpha}{D_B}, \ \ Pr = \frac{\nu}{\alpha}. \tag{12}$$

The non-dimensional BCs from Eqs (5)–(7) becomes

$$\left.\begin{array}{l} f(0) = 0, f'(0) = 1, \phi(0) = 1, \ (0) = 1, \\ f'(\infty) = 0, \theta(\infty) = 0, \phi(\infty) = 0. \end{array}\right\} \tag{13}$$

The heat and mass transfer rates in terms of local Sherwood, the local Nusselt numbers, and the local skin friction coefficient are defined by

$$Sh = \frac{xj_i}{D_B(C_\infty - C_w)}, \ Nu = \frac{xq_i}{K(T_\infty - T_w)}, \ C_f = \frac{2\tau_i}{\rho U_w^2}, \tag{14}$$

where j_i, q_i, and τ_i are the mass, heat, and momentum fluxes from the surface. These are defined as follows:

$$j_i = -D_B\left(\frac{\partial C}{\partial y}\right)_{y=0}, \ \ q_i = -K\left(\frac{\partial T}{\partial y}\right)_{y=0}, \ \ \tau_i = \mu\left(\frac{\partial u}{\partial y}\right)_{y=0} \tag{15}$$

In dimensionless form they are represented as:

$$Re_x^{-\frac{1}{2}}\, Sh = -\sqrt{\frac{X}{2}}\phi'(0), \ \ Re_x^{-\frac{1}{2}}Nu_x = -\sqrt{\frac{X}{2}}\theta'(0), \ \ (2Re)^{\frac{1}{2}}\, C_f = \sqrt{2X}f''(0). \tag{16}$$

Homotopy-Based Approach

The following methodology details should provide as a guide about OHAM aiming to solve nonlinear differential system (9)–(11) with BCs (13) and identify the variations of physical solutions of the differential system. In the framework of OHAM, we can choose auxiliary linear operators in the forms

m	c_0^f	c_0^θ	c_0^ϕ	ε_m^t	t (seconds)
1	-1.02	-0.04	-1.48	0.15×10^{-1}	0.968055
3	-1.19	-0.82	-1.48	0.37×10^{-2}	11.357
5	-1.34	-0.91	-1.56	0.17×10^{-2}	85.337

Table 1. Choice of convergence enhancing parameters for $\beta = N_b = M = N_t = 0.1$, $Le = Pr = 1.0$.

m	10	20	30
ε_m^f	2.07×10^{-7}	1.17×10^{-7}	7.08×10^{-8}
ε_m^θ	0.28×10^{-4}	8.68×10^{-6}	4.77×10^{-6}
ε_m^ϕ	0.62×10^{-3}	0.22×10^{-3}	0.13×10^{-3}
ε_m^t	0.64×10^{-3}	0.23×10^{-3}	2×10^{-3}
t (seconds)	59.2263511	707.5565964	5623.3201208

Table 2. Squared residual errors with $c_0^f = -1.34$, $c_0^\theta = -0.91$, $c_0^\phi = -1.56$ for $\beta = N_b = M = N_t = 0.1$, $Le = Pr = 1.0$.

$$\mathcal{L}_1[u(\eta: q)] = \frac{d^3 u}{d\eta^3} - \frac{du}{d\eta},$$
(17)

$$\mathcal{L}_2[v(\eta: q)] = \frac{d^2 u}{d\eta^2} - v.$$
(18)

Obviously, the operators satisfying the below assumptions

$$\mathcal{L}_1[D_1 \exp(-\eta) + D_2 exp(\eta) + D_3] = 0,$$
(19)

$$\mathcal{L}_2[D_4 \exp(-\eta) + D_5 exp(\eta)] = 0.$$
(20)

The corresponding auxiliary linear operator for $f(\eta)$ is $\mathcal{L}_1$ and $\mathcal{L}_2$ corresponds to $\theta(\eta)$ and $\phi(\eta)$. In OHAM we also have flexibility to pick the initial solutions. It is mandatory that all initial solutions should satisfy the BCs (13). Therefore, we set the initial solutions as follows:

$$f_0(\eta) = 1 - \exp(-\lambda_a \eta),$$
(21)

$$\theta_0(\eta) = \exp(-\lambda_b \eta),$$
(22)

$$\phi_0(\eta) = \exp(-\lambda_b \eta).$$
(23)

where $\lambda_a = \lambda_b = 1$. We have applied BVPh 2.0 to solve nonlinear differential system (9)–(11) with BCs (13). With linear operators (17) and (18) and initial solutions (21)–(23), the Eqs (9)–(11) with BCs (13) can be solved directly by using BVPh 2.0 in quite easy and convenient way.

Results and Discussion

The OHAM approximations contains unknown convergence enhancing parameters c_0^f, c_0^θ and c_0^ϕ. Liao[46] proposed Minimum Error Method that can be used to compute values for convergence enhancing parameters. These optimal convergence control parameters ensure the fast convergence of OHAM solutions. The mechanism for the choice of optimal convergence enhancing parameters is explained by an illustrative example. Let us assume $\beta = N_b = M = N_t = 0.1$, $Le = Pr = \lambda = 1.0$, the optimal values of c_0^f, c_0^θ and c_0^ϕ are computed through the minimization of squared residual error as shown in Table 1. It is noted that the total error is decreased by increasing the order of iteration. Optimal convergence-control parameters corresponding to 5th-order OHAM iteration are then used to check the convergence of our results at various orders of approximation. The OHAM iterations at various orders are shown in Table 2. The presented results demonstrate the high efficiency and reliability of OHAM series solutions. The graphical analysis has been accomplished for the flow pattern, concentration, temperature, the local Sherwood number and the local Nusselt number for various values of β, Le, Pr, M, N_t and N_b.

Figure 2 illustrates the impact of β on the velocity graph for different M. It is visible that fluid flow is maximum in the ambient fluid for smaller β. However, the fluid changes its properties from Newtonian to non-Newtonian characteristics for higher β, and hence the flow shows decreasing behavior. The boundary layer thickness reduces as we increase β and M.

Figure 3 displays the influence of β and M on concentration and temperature graphs. It is observed that the increase in β and M enhances concentration and temperature.
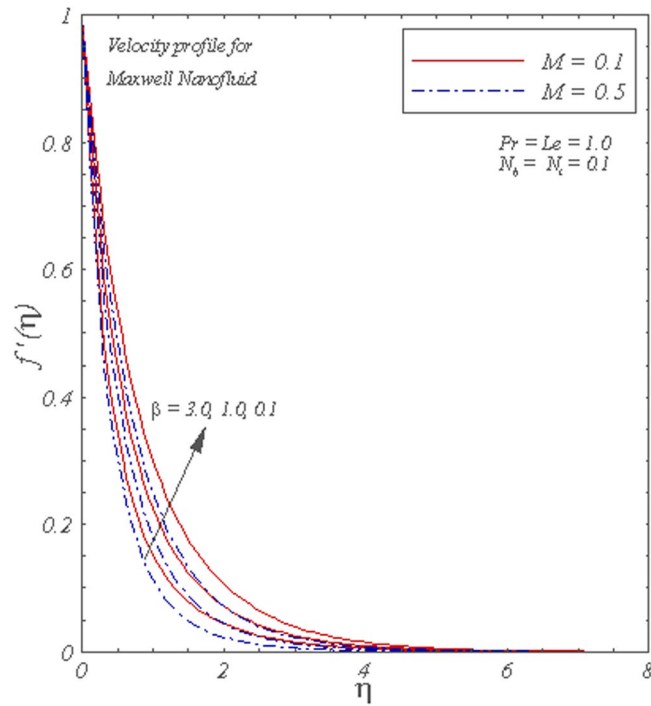
Figure 2. Graphs of $f'(\eta)$ for different β and M.
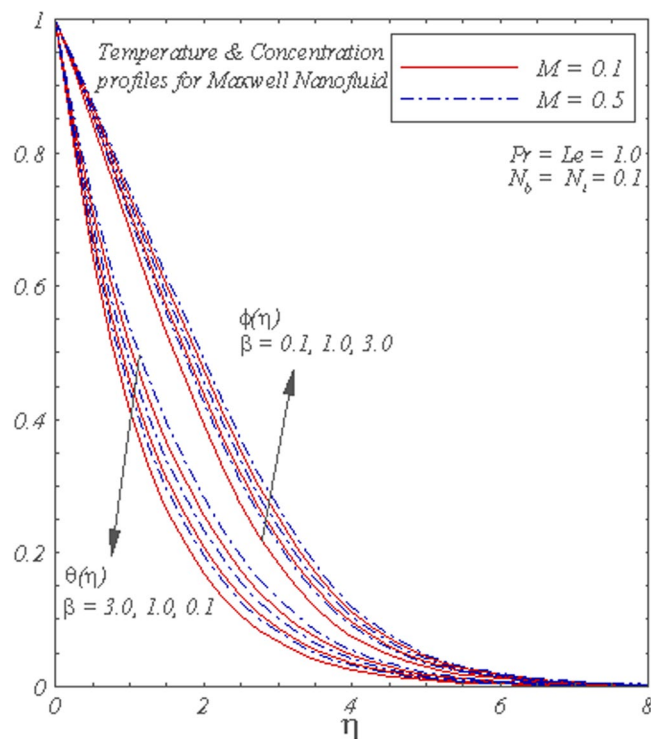
Figure 3. Graphs of $\theta(\eta)$ and $\phi(\eta)$ for different values of β and M.

Figure 4 describes the dimensionless concentration and temperature for various values of N_b. The temperature increases with the increase of N_b but concentration decreases in the boundary layer region.

Figure 5 illustrates that due to increase in the values of N_t, the concentration profile increases but temperature decreases. The overshoot in the concentration is observed that is highest concentration occurs in the ambient fluid but not at the surface.
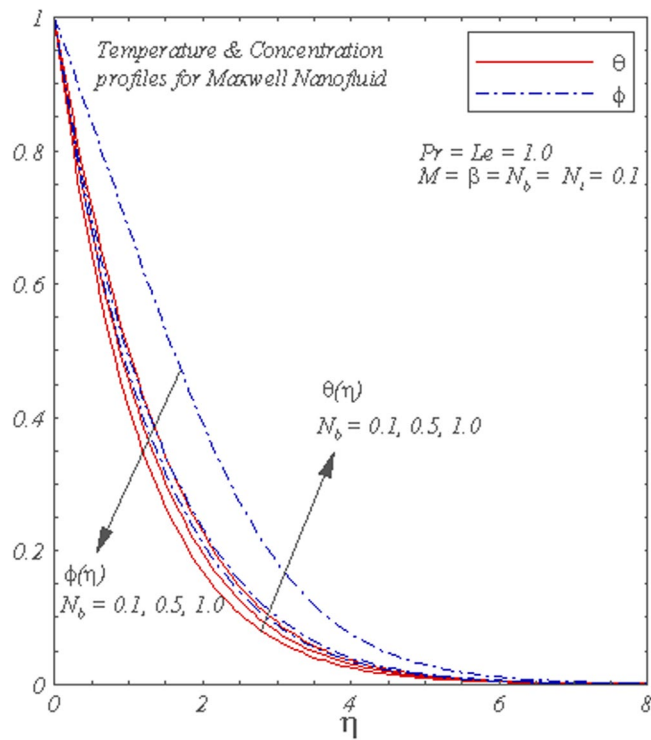
Figure 4. Graphs of $\theta(\eta)$ and $\phi(\eta)$ for different N_b.
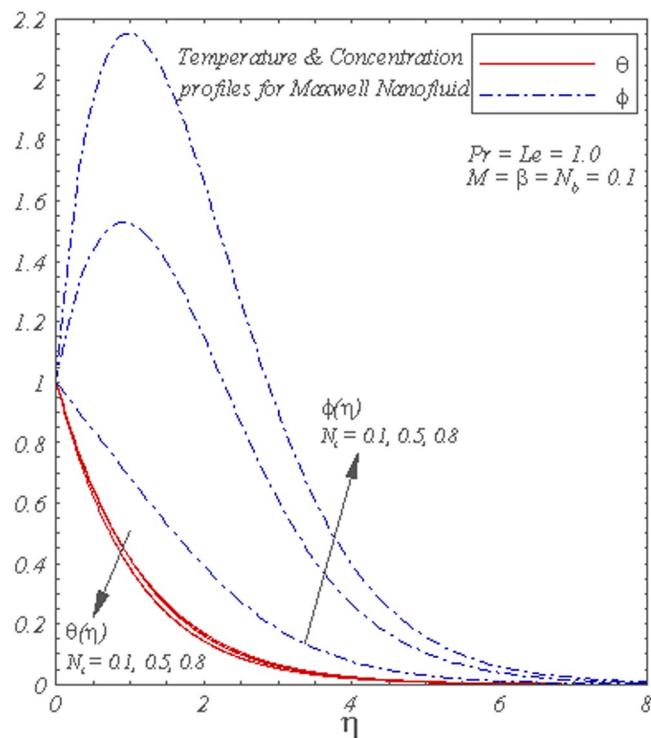
Figure 5. Graphs of $\theta(\eta)$ and $\phi(\eta)$ for different N_t.

Figure 6 describes the influence of Pr on the concentration and temperature profiles. Temperature is a decreasing function of Pr. The dimensionless temperature decreases for higher Pr and hence the thermal boundary layer reduces. Concentration overshoot is observed near the wall.
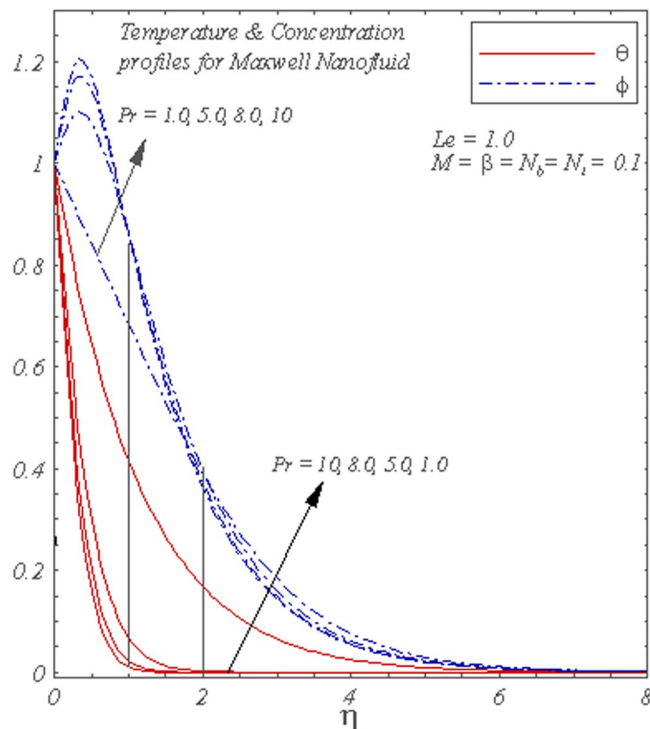
Figure 6. Graphs of $\theta(\eta)$ and $\phi(\eta)$ for different Pr.
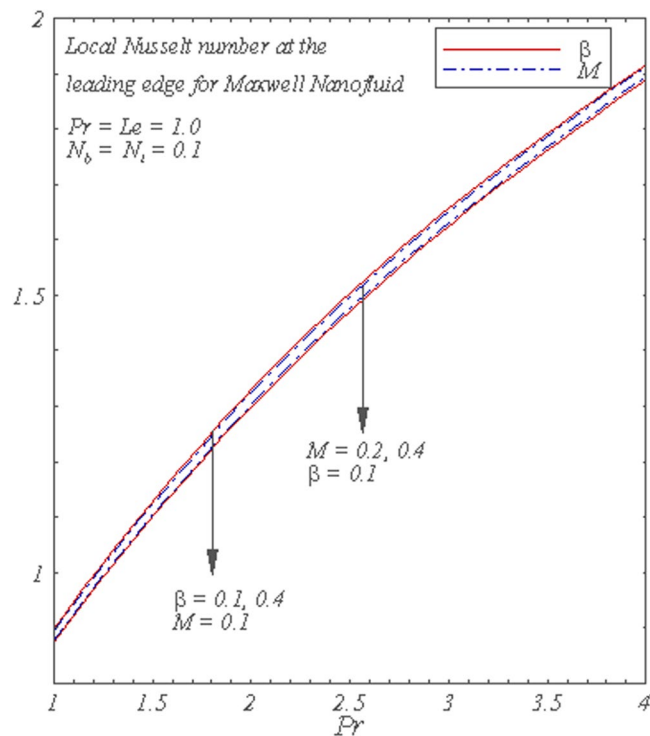
Figure 7. Graphs of the local Nusselt number for Pr with varying M and β.

Figure 7 displays the local Nusselt number for several values of β and M. The local Nusselt number is an increasing function of Pr but the increase in β and M decreases the local Nusselt number.

Figure 8 shows that the local Nusselt number is a decreasing function of N_b. The increase in either N_t or Le decreases the local Nusselt number. The local Sherwood number is plotted as a function of N_b in Fig. 9. It can be seen that local Sherwood number is an increasing function of N_b and Le. However, the increase in N_t decreases the local Sherwood number.
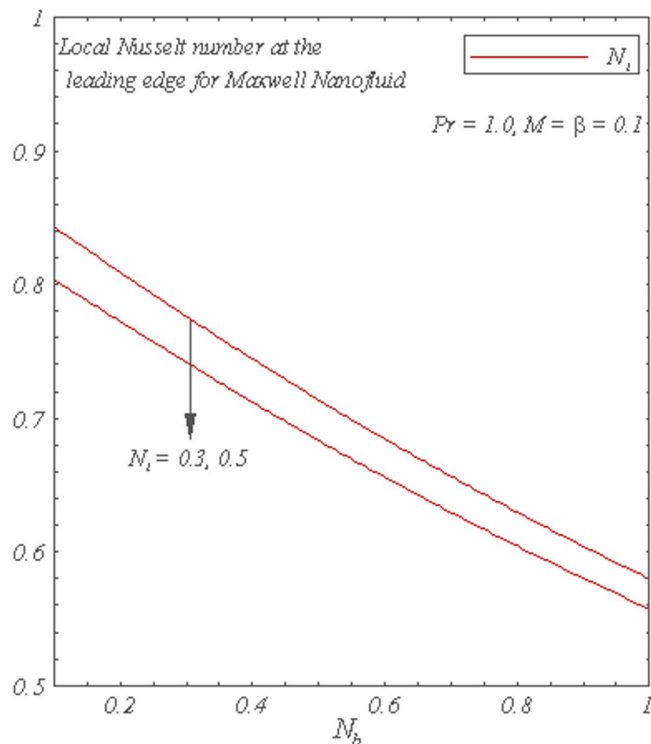
Figure 8. Graphs of the local Nusselt Number for N_b with varying N_t.
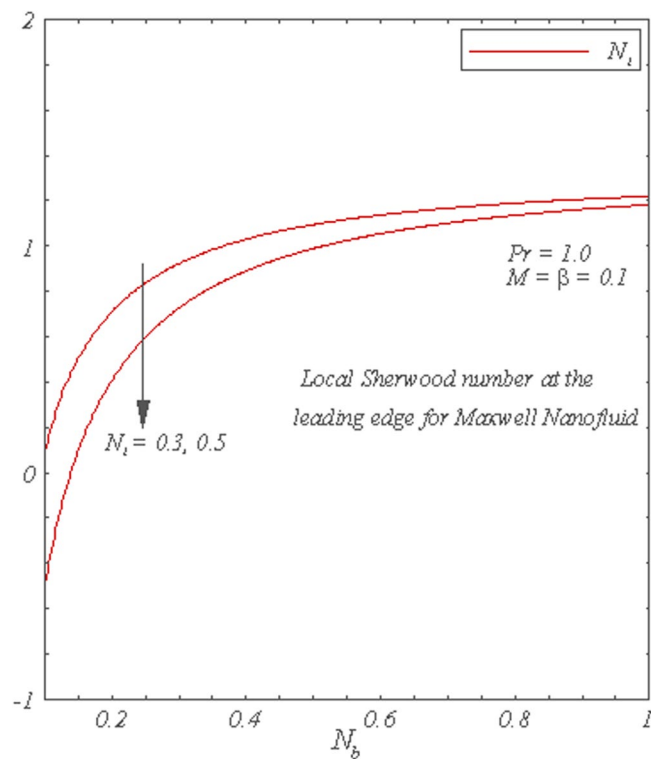
Figure 9. Graphs of the local Sherwood Number for N_b with varying N_t.

Figure 10 exhibits the local skin friction coefficient as a function of Prandtl number. The change in Prandtl number does not affect the local skin friction coefficient. It is also observed the increase in β and M reduces the local skin friction coefficient.
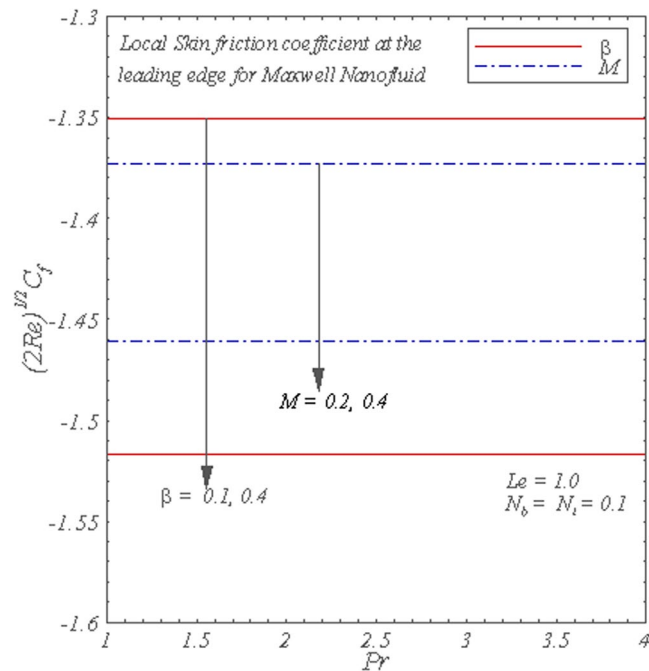
Figure 10. Graphs of the local skin friction coefficient with varying M and β.

Conclusions

The main points of presented analysis are given below.

- Increase in β and M enhances the flow.
- Temperature is enhanced through increase in β, M and N_b whereas it decreases due to increase in N_t and Pr.
- The increase in the values of β, M and N_t leads to an increase in the volumetric concentration profile, whereas quite opposite is true for N_b.
- The local Nusselt number increases with an increase in Pr. However, local Nusselt number decreases with the increase in M, β, L_e and N_t.
- The local Sherwood number is increasing function of N_b and L_e, whereas it decreases for an increase in N_t.

References

1. Sakiadis, B. C. Boundary layer behavior on continuous solid surfaces: I Boundary layer equations for two dimensional and axisymmetric flow. *AIChe J.* **7**(1), 26–28 (1961).
2. Sakiadis, B. C. Boundary layer behavior on continuous solid surfaces: II The boundary layer on a continuous flat surface. *AIChe J.* **7**(2), 221–225 (1961).
3. Sakiadis, B. C. Boundary layer behavior on continuous solid surfaces: III The boundary layer on a continuous cylindrical surface. *AIChe J.* **7**(3), 467–472 (1961).
4. Zheng, L., Wang, L. & Zhang, X. Analytical solutions of unsteady boundary flow and heat transfer on a permeable stretching sheet with non-uniform heat source/sink. *Comm. Nonlin. Sci. Num. Sim.* **16**, 731–740 (2011).
5. Zheng, L., Niu, J., Zhang, X. & Gao, Y. MHD flow and heat transfer over a porous shrinking surface with velocity slip and temperature jump. *Math. Comp. Model.* **56**, 133–144 (2012).
6. Zheng, L., Liu, N. & Zhang, X. Maxwell fluids unsteady mixed flow and radiation heat transfer over a stretching permeable plate with boundary slip and non-uniform heat source/sink. *ASME J. heat. Tran.* **135**, 031705–6 (2013).
7. Magyari, E. & Keller, B. Heat and mass transfer in the boundary layers on an exponentially stretching continuous surface. *J. Phy. D: Appl. Phys.* **32**, 577–585 (1999).
8. Sajid, M. & Hayat, T. Influence of thermal radiation on the boundary layer flow due to an exponentially stretching sheet. *Int. Comm. Heat. Mass. Tran.* **35**, 347–356 (2008).
9. Sahoo, B. & Poncet, S. Flow and heat transfer of a third grade fluid past an exponentially stretching sheet with partial slip condition. *Int. J. Heat. Mass. Tran.* **54**, 5010–5019 (2011).
10. Mukhopadhyay, S. Slip effects on MHD boundary layer flow over an exponentially stretching sheet with suction/blowing and thermal radiation. *Ain. Shams. Eng. J.* **4**(3), 485–491 (2013).
11. Mukhopadhyay, S. MHD boundary layer flow and heat transfer over an exponentially stretching sheet embedded in a thermally stratified medium. *Alex. Eng. J.* **52**(3), 259–265 (2013).
12. Rahman, M. M., Rosca, A. V. & Pop, I. Boundary layer flow of a nanofluid past a permeable exponentially shrinking/stetching surface with second order slip using Buongiorno's model. *Int. J. Heat. Mass. Tran.* **77**, 1133–1143 (2014).
13. Hayat, T., Saeed, Y., Alsaedi, A. & Asad, S. Effects of convective heat and mass transfer in flow of Powell-Eyring fluid past an exponentially stretching sheet. *PLoS One* **10**, e0133831 (2015).
14. Patil, P. M., Latha, D. N., Roy, S. & Momoniat, E. Double diffusive mixed convection flow from a vertical exponentially stretching surface in presence of the visous dissipation. *Int. J. Heat. Mass. Tran.* **112**, 758–766 (2017).
15. Salahuddin, T., Malik, M. Y., Hussain, A., Bilal, S. & Awais, M. Effects of transverse magnetic field with variable thermal conductivity on tangent hyperbolic fluid with exponentially varying viscosity. *AIP Adv.* **5**, 127103 (2015).

16. Hayat, T., Muhammad, T., Shehzad, S. A. & Alsaedi, A. Similarity solution to three-dimensional boundary layer flow of second grade nanofluid past a stretching surface with thermal radiation and heat source/sink. *AIP Adv.* **5**, 017107 (2015).
17. Mustafa, M., Khan, J. A., Hayat, T. & Alsaedi, A. Simulations for Maxwell fluid flow past a convectively heated exponentially stretching sheet with nanoparticles. *AIP Adv.* **5**, 037133 (2015).
18. Awais, M., Hayat, T. & Ali, A. 3-D Maxwell fluid flow over an exponentially stretching surface using 3-stage Lobatto IIIA formula. *AIP Adv.* **6**, 055121 (2016).
19. Hayat, T., Imtiaz, M. & Alsaedi, A. Boundary layer flow of Oldroyd-B fluid by exponentially stretching sheet. *App. Math. Mech.* **37**(5), 573–582 (2016).
20. Ahmad, K., Honouf, Z. & Ishak, Z. Mixed convection Jeffrey fluid flow over an exponentially stretching sheet with magnetohydrodynamic effect. *AIP Adv.* **6**, 035024 (2016).
21. Weidman, P. Flows induced by an exponential stretching shearing plate motions. *Phys. Fluids.* **28**, 113602 (2016).
22. Rehman, S., Haq, R., Lee, C. & Nadeem, S. Numerical study of non-Newtonian fluid flow over an exponentially stretching surface: an optimal HAM validation. *J. Braz. Soc. Mech. Sci. Eng.* **39**, 1589–1596 (2017).
23. Rehman, F., Nadeem, S. & Haq, R. Heat transfer analysis for three-dimensional stagnation-point flow over an exponentially stretching surface. *Chi. J. Phys.* **55**, 1552–1560 (2017).
24. Fetecau, C. & Fetecau, C. A new exact solution for the flow of Maxwell fluid past an infinite plate. *Int. J. Nonlin. Mech.* **38**(3), 423–427 (2003).
25. Wang, Y. & Hayat, T. Fluctuating flow of Maxwell fluid past a porous plate with variable suction. *Nonlin. Analy: Real. World. App.* **9**(4), 1269–1268 (2008).
26. Fetecau, C. Unsteady flow of a generalized Maxwell fluid with fractional derivative due to a constantly accelerating plate. *Comput. Math. Appl.* **57**(4), 596–603 (2009).
27. Hayat, T., Abbas, Z. & Sajid, M. MHD stagnation point flow of an upper-convected Maxwell fluid over a stretching surface. *Chaos. Soliton. Fract.* **39**(2), 840–849 (2009).
28. Heyhyat, M. M. & Khabazi, N. Non-isothermal flow of Maxwell fluids above fixed flat plates under the influence of a transverse magnetic field. *J. Mech. Eng. Sci.* **225**, 909–916 (2010).
29. Hayat, T. & Qasim, M. Influence of thermal radiation and Joule heating on MHD flow of a Maxwell fluid in the presence of thermophoresis. *Int. J. Heat. Mass. Tran.* **53**, 4780–4788 (2010).
30. Jamil, M. & Fetecau, C. Helical flows of Maxwell fluid between coaxial cylinders. *Nonlin. Analy: Real. World. App.* **11**(5), 4302–4311 (2010).
31. Zheng, L., Li, C., Zhang, X. & Gao, Y. Exact solutions for the unsteady rotating flows of a generalized Maxwell coaxial cylinders. *Comput. Math. Appl.* **62**, 1105–1115 (2011).
32. Wang, S. & Tan, W. C. Stability analysis of soret driven double-diffusive convection of Maxwell fluid in a porous medium. *Int. J. Heat. Fluid. Fl.* **32**(1), 88–94 (2011).
33. Motsa, S. S., Hayat, T. & Aldossary, O. M. MHD flow of upper-convected Maxwell fluid over porous stretching sheet using successive Taylor series linearization method. *J. Appl. Math. Mech.* **33**(8), 975–990 (2012).
34. Mukhopadhyay, S. Heat transfer characteristics for the Maxwell fluid flow past an unsteady stretching permeable surface embedded in a porous medium with thermal radiation. *J. Appl. Mech.* **54**(3), 385–396 (2013).
35. Ramesh, G. K., Roopa, G. S., Gireesha, B. J., Shehzad, S. A. & Abbasi, F. M. An electro-magneto-hydrodynamic flow Maxwell nanoliquid past a Riga plate: a numerical study. *J. Braz. Soc. Mech. Sci. Eng.* **39**, 4547–4554 (2017).
36. Khan, M. I., Waqas, M., Hayat, T., Khan, M. I. & Alsaedi, A. Behavior of stratification phenomenon in flow of Maxwell nanomaterial with motile gyrotactic microorganisms in the presence of magnetic field. *Int. J. Mech. Sci.* **131–132**, 426–434 (2017).
37. Khan, M. I., Waqas, M., Hayat, T., Khan, M. I. & Alsaedi, A. Chemically reactive flow of upper-convected Maxwell fluid with Cattaneo-Christov heat flux model. *J. Braz. Soc. Mech. Sci. Eng.* **39**, 4571–4578 (2017).
38. Choi, S. Enhancing thermal conductivity of fluids with nanoparticle in: Siginer, D. A. & Wanf, H. P. (Eds) Developments and applications of non-Newtonian flows, *ASME MD. FED.* **231**, 99–105 (1995).
39. Buongiorna, J. Convective transport in nanofluids. *ASME J. Heat. Tran.* **128**, 240–250 (2006).
40. Mustafa, M., Hayat, T., Pop, I., Asghar, S. & Obaidat, S. Stagnation-point flow of a nanofluid towards a stretching sheet. *Int. J. Heat. Mass. Tran.* **54**, 5588–5594 (2011).
41. Rashidi, M. M., Abelman., S. & Freidoonimehr, N. Entropy generation steady MHD flow due to a rotatintg porous media disk in a nanofluid. *Int. J. Heat. Mass. Tran.* **62**, 515–525 (2013).
42. Turkyilmazoglu, M. Unsteady convection flow of some nanofluids past a moving vertical plate plate with heat transfer. *ASME J. Heat. Tran.* **136**(3), 031704 (2013).
43. Rashidi, M. M., Kavyani, N. & Abelman, S. Investigation of entropy generation in MHD and slip flow over a rotating porous disk with variable properties. *Int. J. Heat. Mass. Tran.* **70**, 892–917 (2014).
44. Sheikholeslami, M., Rashidi, M. M. & Ganji, D. D. Effect of non-uniform magnetic field on forced convection heat transfer of Fe_3O_4-water nanofluid. *Comput. Method. Appl. M.* **294**, 299–312 (2015).
45. Sheikholeslami, M., Vajravelu, K. & Rashidi, M. M. Forced convection heat transfer in a semi annulus under the influence of a variable magnetic field. *Int. J. Heat. Mass. Tran.* **92**, 339–348 (2016).
46. Liao, S. An optimal homotopy analysis approach for strongly nonlinear differential equations. *Comm. Nonlin. Sci. Num. Sim.* **15**(8), 2003–2016 (2010).
47. Farooq, U., Zhao, Y. L., Hayat, T., Alsaedi, A. & Liao, S. J. Application of the HAM-Based Mathematica Package BVPh2.0 on MHD Falkner-Skan flow of nanofluid. *Comput. Fluids.* **111**, 69–75 (2015).
48. Zhong, X. & Liao, S. Analytic solutions of Von Karman plate under arbitrary uniform pressure (I): Equations in differential form. *Stud. Appl. Math.* **138**(4), 12158 (2016).
49. Zhong, X. & Liao, S. On the homotopy analysis method for backward/forward-backward stochastic differential equations. *Numer. Algorithms.* **76**(2), 487–519 (2016).
50. Zhong, X. & Liao, S. Analytic Approximations of Von Karman Plate under Arbitrary Uniform Pressure — Equations in Integral Form. *SCI. CHINA. Phys. Mech.* **61**, 014611 (2018).

Acknowledgements

Author Contributions

S.M. and U.F. wrote the main manuscript text. M.R. and M.S. performed the mathematical modeling. S.H. and D.C.L. prepared the figures and tables. All authors reviewed the manuscript.

Additional Information

Competing Interests: The authors declare no competing interests.

Publisher's note: Springer Nature remains neutral with regard to jurisdictional claims in published maps and institutional affiliations.